



Magnetocaloric effect in HoMnO₃ crystal

A. Midya, P. Mandal, S. Das, S. Banerjee, L. S. Sharath Chandra, V. Ganesan, and S. Roy Barman

Citation: *Applied Physics Letters* **96**, 142514 (2010); doi: 10.1063/1.3386541

View online: <http://dx.doi.org/10.1063/1.3386541>

View Table of Contents: <http://scitation.aip.org/content/aip/journal/apl/96/14?ver=pdfcov>

Published by the [AIP Publishing](#)

Articles you may be interested in

Refrigerant capacity and direct measurements of the magnetocaloric effect on LaFe_{11.2}Co_{0.7}Si_{1.1}C_x materials

J. Appl. Phys. **107**, 09A933 (2010); 10.1063/1.3349372

Large magnetic refrigerant capacity in Gd₇₁Fe₃Al₂₆ and Gd₆₅Fe₂₀Al₁₅ amorphous alloys

J. Appl. Phys. **105**, 053908 (2009); 10.1063/1.3072631

Composition dependence of magnetocaloric effect in Sm_{1-x}Sr_xMnO₃ (x = 0.3 – 0.5)

Appl. Phys. Lett. **93**, 232501 (2008); 10.1063/1.3040698

Oxygen deficiency as a driving force for metamagnetism and large low field magnetocaloric effect in La_{0.7}Ca_{0.3-x}Sr_xMnO₃ manganites

J. Appl. Phys. **104**, 113916 (2008); 10.1063/1.3040153

Magnetocaloric effect in Ho₅Pd₂: Evidence of large cooling power

Appl. Phys. Lett. **91**, 082511 (2007); 10.1063/1.2775050

The logo for AIP Chaos is displayed on a red background with a geometric, faceted pattern. The letters 'AIP' are in a large, white, sans-serif font, followed by a vertical line and the word 'Chaos' in a smaller, white, sans-serif font.

AIP | Chaos

CALL FOR APPLICANTS
Seeking new Editor-in-Chief

Magnetocaloric effect in HoMnO₃ crystal

A. Midya,¹ P. Mandal,^{1,a)} S. Das,¹ S. Banerjee,¹ L. S. Sharath Chandra,² V. Ganesan,² and S. Roy Barman²

¹Saha Institute of Nuclear Physics, 1/AF Bidhannagar, Calcutta 700064, India

²UGC-DAE Consortium for Scientific Research, Khandwa Road, Indore 452001, India

(Received 21 January 2010; accepted 19 March 2010; published online 9 April 2010)

We have investigated the magnetic and magnetocaloric properties of HoMnO₃ single crystal. HoMnO₃ displays a series of complicated phase transitions due to the long range ordering of Mn³⁺ and Ho³⁺ moments. Field variation in magnetization generates a metamagnetic transition and produces an entropy change of 13.1 J/kg K at 7 T in the vicinity of antiferromagnetic ordering temperature of Ho³⁺. The values of adiabatic temperature change (~6.5 K) and relative cooling power (~320 J/kg) for a field change of 7 T are also appreciable to consider HoMnO₃ as a magnetic refrigerant at low temperature. © 2010 American Institute of Physics.

[doi:10.1063/1.3386541]

Magnetocaloric effect (MCE) describes the reversible change in temperature (ΔT_{ad}) of a magnetic material under adiabatic condition produced by the magnetic entropy change ΔS_M due to the variation in applied magnetic field.¹ MCE becomes maximum close to the paramagnetic to ferromagnetic transition temperature.¹ In the case of first order magnetic transition,^{2,3} a large entropy change ΔS_M originates from the difference in the degree of magnetic ordering between two adjacent magnetic phases arising from the coupling of magnetic spin system of the solid with the external applied magnetic field and as a consequence a large MCE is observed. Magnetic refrigeration, based on the MCE, has attracted much research interest due to its potential advantage of the higher energy efficiency and environmental friendliness over the conventional vapor compression refrigeration. Previous studies on MCE were concentrated mainly on rare earth elements and their alloys and intermetallic compounds with high total angular momentum quantum number such as Gd,¹ Gd₅Si₂Ge₂,² and RAl₂ (R=Dy, Ho, and Er).⁴ Large MCE has also been observed in some Mn-based alloys and compounds^{3,5,6} and in some ferromagnetic colossal magnetoresistive manganites.^{1,7,8} Researches are in progress in search of new materials which have large MCE at low fields close to room temperature for domestic and other technological applications. On the other hand, systems showing large MCE in the low-temperature region from about 30 K down to sub-Kelvin are also important for basic research as well as for specific technological applications such as space science and liquification of hydrogen in fuel industry.^{1,9} Recently the rich physics and the prospects for practical application involved in multiferroic rare earth manganites have evoked considerable research activity.¹⁰⁻¹² However, the magnetocaloric nature of these materials and their potentials for application in magnetic refrigeration have not been investigated yet.

In hexagonal HoMnO₃, the Mn³⁺ moments occupy a fully frustrated triangular sublattice in the plane, which are then stacked in alternating fashion along the *c* axis with Ho³⁺ layers in between. The Ho–O displacements give rise to a ferroelectric moment along the *c* axis ($T_C=875$ K) and the

Mn³⁺ moments order at the Neel temperature $T_{N1} \sim 72$ K. At $T_{SR} \sim 40$ K, a Mn³⁺ spin reorientation transition takes place where the Mn moments rotate in plane by an angle of 90°. This transition is followed by a partial ordering of the Ho spins along the *c* direction. Below $T_{N2} \sim 5$ K, the magnetic moment of the Ho³⁺ ion is completely ordered.¹³⁻¹⁶ The ordering nature of the Ho-spin has not been resolved yet. The large field-induced magnetization observed in HoMnO₃ has motivated us to investigate the magnetocaloric behavior in this system. Here we present a comprehensive study of the magnetocaloric effect of HoMnO₃ measured on single crystal near the Ho-spin ordering transition.

Polycrystalline HoMnO₃ was prepared from stoichiometric mixture of Ho₂O₃ and Mn₃O₄ by solid state reaction and the single crystal was grown from the powders using traveling solvent floating zone image furnace. Magnetization measurements were carried out employing a superconducting quantum interference device magnetometer (Quantum Design). Magnetization (*M*) isotherms were taken at a temperature interval (ΔT) of 1–2 K in the range between 2–12 K and 12–40 K, respectively. The specific heat measurement was performed using a Quantum Design physical property measurement system. The x-ray diffraction pattern of powdered sample of single crystal reveals that the sample is single phase with hexagonal P6₃cm structure.

Figure 1 shows the thermal variation in the susceptibility $\chi (=M/H)$ of HoMnO₃ crystal measured at a magnetic field $H=4$ Oe. The susceptibility strongly increases with the decrease in the temperature. In the upper inset, we have shown zero field cooled (ZFC) and field cooled (FC) curves in the low-temperature region below 50 K. Near about 4.5 K both the curves show an anomaly with a sudden increase in magnetization with decreasing *T*. This abrupt change corresponds to the antiferromagnetic (AFM) ordering of Ho³⁺ moments. A second anomaly is observed near about 40 K below which the FC and ZFC curves bifurcate (shown in the lower inset). This irreversibility arises due to the reorientation of Mn³⁺ and/or Ho³⁺ spins in domain boundaries.¹⁷ No anomaly is detected at the Neel temperature T_{N1} corresponding to the AFM ordering of the Mn³⁺ moments. In the mainframe of the figure, we have also plotted the inverse susceptibility against temperature. The linearity of the curve above 80 K

^{a)}Electronic mail: prabhat.mandal@saha.ac.in.

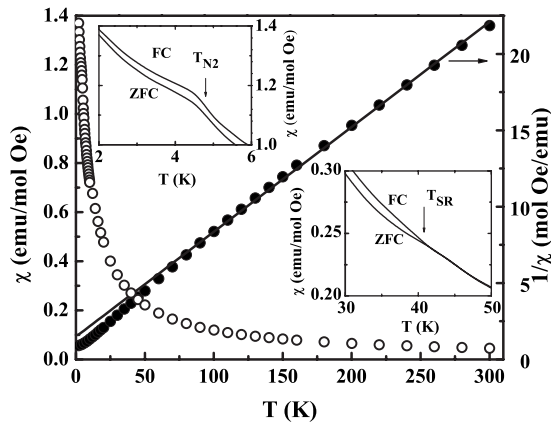


FIG. 1. Temperature dependence of χ ($H=4$ Oe) and $1/\chi$: Upper inset: ZFC and FC curves of $\chi(T)$ near the AFM transition of Ho^{3+} . Lower inset: ZFC and FC curves of $\chi(T)$ near the spin reorientation transition of Mn^{3+} .

reveals that $\chi(T)$ follows the Curie–Weiss law [$\chi=C/(T-\theta)$] in that temperature regime. Fitting the experimental data, we get the Curie–Weiss temperature, $\theta=-21$ K. The estimated effective moment $P_{\text{eff}}=11.1 \mu_B$ is consistent with the theoretically expected value of $11.7 \mu_B$. The thermal evolution of heat capacity C_p under zero magnetic field, depicted in Fig. 2, presents three distinct transitions in the whole temperature range. The λ -type anomaly at 71 K suggests the AFM ordering of the Mn^{3+} magnetic moments. A small peak at $T_{\text{SR}}=39$ K (enlarged in the inset) indicates the Mn spin reorientation. Besides these two peaks, there exists another prominent peak at $T_{\text{N}2}=4.6$ K which marks the AFM transition of Ho^{3+} moments. Absence of any anomaly at $T_{\text{N}1}$ in the χ versus T curve is often explained as the suppression due to the large paramagnetic susceptibility of the Ho^{3+} ions.¹⁸ Some representative plots of isothermal field variation in magnetization of HoMnO_3 for temperatures 2–40 K are presented in Fig. 3 which upholds a field-induced metamagnetic transition. The magnetic field for each isotherm has been varied between zero and 7 T, and the field is applied nearly parallel to the c axis. The isotherms vary almost linearly with the field in the low-field region and depending upon the temperature the slope changes at a critical field without any indication of saturation. Inset of Fig. 3 displays the five-segment $M(H)$ curve of HoMnO_3 at 2 K and the curve shows a negligible hysteresis effect.

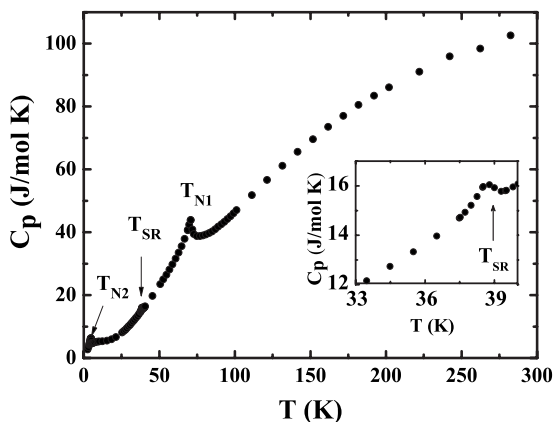


FIG. 2. Heat capacity of HoMnO_3 as a function of temperature at zero magnetic field. Inset presents the spin reorientation transition of Mn^{3+} .

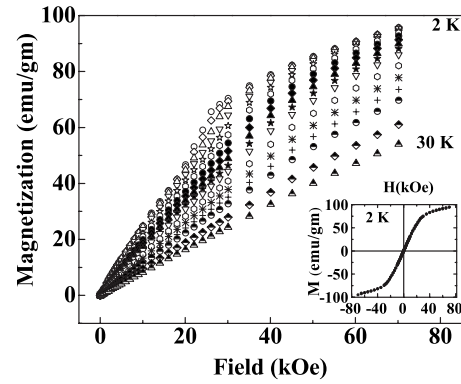


FIG. 3. Representative M - H isotherms of HoMnO_3 measured at different temperatures near the Ho-spin ordering transition (from 2–12 K with $\Delta T=1$ K, from 14–20 K with $\Delta T=2$ K, and from 25–30 K with $\Delta T=5$ K); Inset shows the hysteresis at 2 K.

The magnetic entropy change (ΔS_M) associated with the magnetocaloric effect, can be calculated from the magnetization data using the Maxwell relation¹ $\Delta S_M(T, H) = \int_0^H (\partial M / \partial T)_H dH$. It can also be determined from the specific heat data using the relation

$$\Delta S_M(T, H) = \int_0^T \frac{C_p(H) - C_p(0)}{T} dT, \quad (1)$$

where $C_p(0)$ and $C_p(H)$ are heat capacity without magnetic field and with magnetic field, respectively. The value of ΔS_M was determined from the isothermal magnetization curves obtained at different temperatures (Fig. 3) with an appropriate interval of temperature ΔT . The area enclosed by the two isotherms at temperatures T_1 and T_2 is divided by $\Delta T=T_2-T_1$ to determine ΔS_M at the average temperature $T=(T_1+T_2)/2$. Figure 4 displays the entropy change as a function of temperature for the field variation from 0–1 to 0–7 T. The curves present a characteristic shape with a broad maximum in the vicinity of the AFM transition of Ho moment and the width enhances as the magnetic field increases. It may be noted that the $-\Delta S_M$ maximum in Fig. 4 does not coincide with the transition temperature. The position of the maximum shifts from 5.5 to 9.5 K when the magnetic field change (ΔH) increases from 1 to 7 T. The magnitude of $-\Delta S_M$ at maximum increases linearly with increasing magnetic field up to -13.1 J/kg K at 7 T. The field-induced metamagnetic transition contributes to the enhancement of ΔS_M . Now the

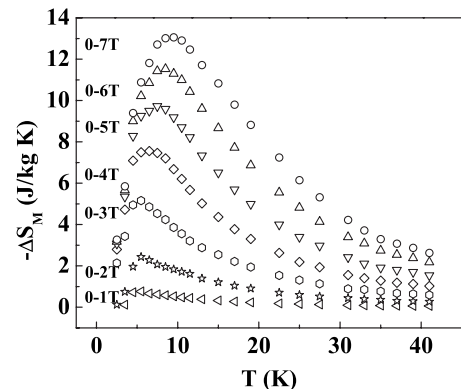


FIG. 4. Magnetic entropy change ΔS_M of HoMnO_3 (calculated from M - H curve) as a function of temperature for a field variation from 0–1 to 0–7 T.

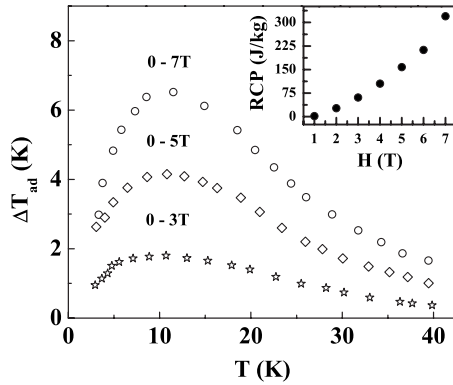


FIG. 5. The adiabatic temperature change (ΔT_{ad}) in HoMnO_3 .

total entropy $S(0, T)$ under zero magnetic field can be calculated from the heat capacity data as

$$S(0, T) = \int_0^T \frac{C(0, T)}{T} dT, \quad (2)$$

and then the entropy under magnetic field, $S(H, T)$, is determined by subtracting the corresponding ΔS_M from $S(0, T)$. The adiabatic temperature difference ΔT_{ad} is obtained from the isentropic difference between the entropy curves $S(0, T)$ and $S(H, T)$.² The temperature dependence of ΔT_{ad} is plotted in Fig. 5 for different fields. The peak of the curve corresponds to $\Delta T_{ad} = 6.5$ K for a field change of 7 T. In addition to the values of ΔS_M and ΔT_{ad} the relative cooling power (RCP) is also evaluated to determine the cooling efficiency of a magnetocaloric material. RCP based on the magnetic cooling power is defined as the product of ΔS_M maximum and the full width at half maximum δT_{FWHM} of $\Delta S_M(T)$ curve as $\text{RCP} = \Delta S_M \times \delta T_{FWHM}$. In the inset of Fig. 5, we have presented RCP as a function of magnetic field. RCP is large and increases with the increase in field. Therefore, the magnetocaloric nature of HoMnO_3 satisfies some important criteria for selecting magnetic refrigerants such as exhibition of large magnetic entropy change, large adiabatic temperature change, high RCP value and very small thermal hysteresis. These properties make HoMnO_3 a promising candidate as refrigerant at low temperature. In comparison with the perovskite manganites which exhibit both second order and first order ferromagnetic to paramagnetic phase transition, ΔS_M of the present material is higher at a moderate field

change.^{1,7,8} Moreover, the high electrical resistivity of HoMnO_3 generates a lower value of eddy current loss and hence reduces the cost. It is noteworthy that the magnetization increases largely if the field is applied along the a direction^{14,17} and in that case a larger magnetocaloric effect may be obtained.

To summarize, from the magnetization and heat capacity measurements it is found that HoMnO_3 experiences three magnetic transitions within the temperature range of 2–300 K such as antiferromagnetic transitions of Mn^{3+} and Ho^{3+} moments and a spin reorientation transition of Mn^{3+} moment. A magnetic entropy change ~ 13.1 J/kg K is obtained for a field change of 0–7 T whereas the adiabatic temperature change and RCP are ~ 6.5 K and ~ 320 J/kg, respectively. Considering these data and some practical importance mentioned above HoMnO_3 may be considered as a candidate for magnetic refrigerant at low temperatures.

¹K. A. Gschneidner, Jr., V. K. Pecharsky, and A. O. Tsokol, *Rep. Prog. Phys.* **68**, 1479 (2005), and references therein.

²V. K. Pecharsky and K. A. Gschneidner, Jr., *Phys. Rev. Lett.* **78**, 4494 (1997).

³H. Wada and Y. Tanabe, *Appl. Phys. Lett.* **79**, 3302 (2001).

⁴T. Hashimoto, T. Kuzuhara, M. Sahashi, K. Inomata, A. Tomokiyo, and H. Yayama, *J. Appl. Phys.* **62**, 3873 (1987).

⁵F. Hu, B. Shen, and J. Sun, *Appl. Phys. Lett.* **76**, 3460 (2000).

⁶O. Tegus, E. Brück, K. H. J. Buschow, and F. R. deBoer, *Nature (London)* **415**, 150 (2002).

⁷M. Phan and S. Yu, *J. Magn. Magn. Mater.* **308**, 325 (2007), and references therein.

⁸P. Sarkar, P. Mandal, and P. Choudhury, *Appl. Phys. Lett.* **92**, 182506 (2008).

⁹V. Provenzano, J. Li, T. King, E. Canavan, P. Shirron, M. DiPirro, and R. D. Shull, *J. Magn. Magn. Mater.* **266**, 185 (2003).

¹⁰W. Eerenstein, N. D. Mathur, and J. F. Scott, *Nature (London)* **442**, 759 (2006).

¹¹S.-W. Cheong and M. Mostovoy, *Nature Mater.* **6**, 13 (2007).

¹²M. Fiebig, *J. Phys. D* **38**, R123 (2005).

¹³H. Sugie, N. Iwata, and K. Kohn, *J. Phys. Soc. Jpn.* **71**, 1558 (2002).

¹⁴B. Lorenz, F. Yen, M. M. Gospodinov, and C. W. Chu, *Phys. Rev. B* **71**, 014438 (2005).

¹⁵B. Lorenz, A. P. Litvinchuk, M. M. Gospodinov, and C. W. Chu, *Phys. Rev. Lett.* **92**, 087204 (2004).

¹⁶O. P. Vajk, M. Kenzelmann, J. W. Lynn, S. B. Kim, and S.-W. Cheong, *Phys. Rev. Lett.* **94**, 087601 (2005).

¹⁷E. Galstyan, B. Lorenz, K. S. Martirosyan, F. Yen, Y. Y. Sun, M. M. Gospodinov, and C. W. Chu, *J. Phys.: Condens. Matter* **20**, 325241 (2008).

¹⁸A. Muñoz, J. A. Alonso, M. J. Martínez-Lope, M. T. Casáis, J. L. Martínez, and M. T. Fernández-Díaz, *Chem. Mater.* **13**, 1497 (2001).